

# ACCEPTED VERSION

Adam J. Gee, Yilong Yin, Kae Ken Foo, Alfonso Chinnici, Neil Smith, Paul R. Medwell  
**Toluene addition to turbulent H<sub>2</sub>/natural gas flames in bluff-body burners**  
International Journal of Hydrogen Energy, 2022; 47(65):27733-27746

© 2022 Hydrogen Energy Publications LLC. Published by Elsevier Ltd. All rights reserved.

This manuscript version is made available under the CC-BY-NC-ND 4.0 license  
<http://creativecommons.org/licenses/by-nc-nd/4.0/>

Final publication at: <http://dx.doi.org/10.1016/j.ijhydene.2022.06.154>

## PERMISSIONS

<https://www.elsevier.com/about/policies/sharing>

Accepted Manuscript

Authors can share their [accepted manuscript](#):

24 Month Embargo

### After the embargo period

- via non-commercial hosting platforms such as their institutional repository
- via commercial sites with which Elsevier has an agreement

In all cases [accepted manuscripts](#) should:

- link to the formal publication via its DOI
- bear a CC-BY-NC-ND license – this is easy to do
- if aggregated with other manuscripts, for example in a repository or other site, be shared in alignment with our [hosting policy](#)
- not be added to or enhanced in any way to appear more like, or to substitute for, the published journal article

**13 August 2024**

<http://hdl.handle.net/2440/135791>

# Toluene addition to turbulent H<sub>2</sub>/natural gas flames in bluff-body burners

Adam J. Gee<sup>1,\*</sup>, Yilong Yin<sup>1</sup>, Kae Ken Foo<sup>1</sup>, Alfonso Chinnici<sup>1</sup>, Neil Smith<sup>2</sup> and Paul R. Medwell<sup>1</sup>

<sup>1</sup> *School of Mechanical Engineering, The University of Adelaide, Adelaide, SA 5005, Australia*

<sup>2</sup> *School of Chemical Engineering and Advanced Materials, The University of Adelaide, Adelaide, SA 5005, Australia*

## **Abstract**

A key challenge in the transition towards using hydrogen as an alternative carbon-free fuel is the reduced thermal radiation due to the absence of soot. A novel solution to this may be doping with highly sooting bio-oils. This study investigates the efficacy of toluene as a prevapourised dopant in turbulent pure hydrogen and blended hydrogen/natural gas flames as a means of improving soot loading and radiant heat transfer. All flames are stabilised on bluff-body burners to emulate the recirculation component of many industrial combustors. Total heat flux and illuminance increase non-linearly with toluene concentration for fuel blends and bluff-body diameters. By reducing the bluff-body diameter from 64 mm to 50 mm, a 20/80 (vol%) H<sub>2</sub>/natural gas mixture produces a more radiative flame than a 10/90 H<sub>2</sub>/natural gas mixture in the smaller bluff-body. Opposed-flow flame simulations of soot precursors indicate that as strain rate increases, although overall soot precursor concentration decreases, a 20 vol% hydrogen mixture will produce more soot than a 10 vol% mixture. This suggests the addition of hydrogen up to 20 vol% may be beneficial for soot production in high strain environments.

## **Keywords**

Hydrogen, Toluene, Radiation, Bluff-Body, Doping

## **1 Introduction**

As the world shifts towards renewable sources of energy, the importance of combustion has become apparent for applications that cannot readily be replaced by electrification [1]. Interest in hydrogen (H<sub>2</sub>) as an alternative to natural gas (NG) to fuel the combustion needs of industrial heating has grown considerably in recent years [2, 3]. The characteristics of hydrogen flames have been studied extensively and the benefits of hydrogen combustion are widely documented. The main benefits of hydrogen are a potentially 100% renewable production process [4] with carbon-free emission. A hydrogen flame has increased stability due to its increased flame speed and wider flammability limits [5, 6]. Although currently not a cost-effective alternative, it is expected that green hydrogen, via water electrolysis from renewable electricity, will soon become cost-competitive and become a more attractive carbon-free heat energy source for industrial processes [7]. In this way, hydrogen can be used as an energy storage medium by generating it when there is excess renewable electricity supply. The potential role for hydrogen in energy networks is well established, with the focus now shifting towards solutions to the variety of challenges associated with the integration of a new fuel in existing gas and energy infrastructure.

The challenges associated with the integration of hydrogen in industry applications are not only economic but also related to its performance. The challenges associated with the complete replacement of all current fuels for hydrogen are perhaps too great, but there is a growing interest in understanding the feasibility of blending hydrogen with existing fuels in various applications. When the fuel composition is changed, so too are the resulting flame characteristics, which can have a significant effect on performance and safety. The design and use of a burner assumes the use of a fuel with specific properties, such as natural gas. The addition of a new reacting species in hydrogen has a significant

\* Corresponding author:

Email: [adam.gee@adelaide.edu.au](mailto:adam.gee@adelaide.edu.au)

effect on differential diffusivity, reaction kinetics and, combined with factors affected by varying burner geometries, makes predicting the consequences of hydrogen blending difficult [8]. The reduced radiant heat transfer of hydrogen due to lack of soot is of particular concern with regard to burner thermal efficiencies and although the reduced thermal radiation of hydrogen flames is well documented [9-14] there is still a gap in the knowledge about the extent to which the content of hydrogen in a particular fuel blend will affect performance parameters such as radiant heat transfer in different burner systems. This is especially relevant for adoption strategies, which may follow a gradual integration of hydrogen as a growing component of an existing fuel mixture where sooting fuels are ‘diluted’ and the resulting magnitude of radiative heat transfer becomes affected to an unknown degree [15].

In hydrocarbon-based fuels, the major contributor to radiative heat transfer is the reradiating of thermal energy from soot particles, with gases such as water molecules ( $H_2O$ ) and carbon dioxide ( $CO_2$ ) also contributing [16]. The notion to increase soot is counterintuitive from a health and environmental standpoint and certainly soot poses a risk to those areas but its role in radiant heat transfer is critical to many combustion applications [16, 17]. Soot particles are more efficient emitters than gaseous species and are responsible for the majority of thermal radiation in most hydrocarbon flames [17-19]. The concentration of soot particles is closely coupled to radiant heat losses of a flame [20]. In the combustion of hydrogen flames, there is no carbon present and hence, no soot production. The presence of hydrogen therefore affects a flame’s thermal radiation, since soot particles are important heat carriers [13, 21]. Thermal radiation is the primary mode of heat transfer for many large-scale burner systems [22, 23] thus a lack of soot production and subsequent reduction in thermal radiation would be detrimental to their operation with hydrogen. Direct-fired industrial processes that operate at very high temperatures, such as rotary and glass kilns, boilers and process heaters are particularly reliant on radiation. Additionally, many industry burner systems utilize highly turbulent combustion regimes, the analysis of which with respect to sooting flames is far less prevalent than for laminar flames [24]. Soot is also responsible for much of the visible emissions in hydrocarbon flames due to the blackbody radiation from soot [16, 25]. Consequently, hydrogen flames are often reported as having very poor visibility [26]. The need for solutions to improve the visibility of hydrogen flames is often mentioned as part of a safe adoption strategy of hydrogen for both industrial and domestic use [27]. For cases where hydrogen is blended with a hydrocarbon fuel, the thermal radiation is affected by more than simple dilution of carbon-based species: competing chemical and thermal effects have also been reported [28]. Studies comparing the addition of hydrogen with the addition of inert species for laminar [29, 30] and turbulent [31] flames report that, despite global reductions in soot volume fractions, hydrogen is less effective than inert species at suppressing soot formation, suggesting a chemical promoting effect. Other operating parameters such as the oxygen ( $O_2$ ) concentration [32], and the recirculation rate [33] are known to affect the physical and chemical interactions of blended fuels. The degree to which these interactions affect burner performance for various amounts of hydrogen is a risk faced by industry. Reduced radiative heat transfer [30, 31, 34], lower flame visibility [26], reduced air requirements [35], increased flue gas moisture content and increased NOx emissions [36-40] are some of the key points of concern associated with hydrogen integration to fossil fuel processes.

Extensive efforts have been made to characterise the effect of hydrogen addition in a variety of burners and propose solutions to typical challenges of hydrogen. Kumar and Mishra [13] showed that for hydrogen addition to an LPG diffusion flame there is a negligible effect on flame length for up to 20 vol% hydrogen but a noticeable effect beyond this point. Hydrogen addition up to 40 vol% increased the soot-free-length by approximately 61%, and consequently a negative effect on radiant heat transfer fraction is reported. Kashir et al. [21, 41] has previously investigated the accuracy of model prediction both for the characteristics of methane/hydrogen bluff-body swirl flames [41] and the impact of hydrogen enrichment and bluff-body diameter for propane flames [21]. The authors report the increasing effects of reducing bluff-body diameter on flame length, attributed to the lower recirculation intensity and subsequent reduction in mixing of reactants. In this work the authors considered fractions of hydrogen ranging from 10-70 vol% [41] and 30-90 vol% [21], respectively. In the former case [41]

key features reported were an increase in OH mass fraction and subsequent reaction zone thickness with hydrogen addition. Due to conservation of total volumetric flow rate a penalty is paid on mass flow and thermal input, subsequently the flame temperature was reported to reduce with hydrogen addition — the peak flame temperature was also shifted downstream. In the latter case [21] hydrogen addition decreased radiant heat transfer, consistent with previous experimental data [13] — this was stated to be primarily a consequence of sooting-containing fuels. Adding a dopant to poorly radiating flames has been discussed as a potential solution to improve radiant heat transfer [19]. By doping the flame with particles that emulate the radiant properties of soot, it might be possible to supplement lost radiant heat transfer. The addition of non-combusting metal oxide particles has been proposed as a solution to improve thermal radiation in low sooting flames, [42, 43]. Combustible particles such as pulverised coal and some waste-fuels have also been used as a soot surrogate to improve radiative heat transfer [19, 44]. The recent investigation by Evans et al. [45] on the use of liquid dopants in hydrogen flames has shown merit for toluene, as a representative for the broad family of bio-oils. Toluene is an aromatic compound that is present in the chemical structure of most bio-oils with a high sooting propensity, which is greater than that of petroleum-derived fuels [45–47]. Toluene was added at 1–5 mol% of fuel in 1:1 H<sub>2</sub>:N<sub>2</sub> turbulent (Re = 5000) simple jet flames [45]. The results showed a positive non-linear relationship between the dopant concentration and soot formation. The method of toluene injection, either as a spray or prevapourised, was also found to be an important factor. Computational analysis via OPPDIF models of the sooting characteristics of toluene showed competing chemical pathways for oxidation via formaldehyde (CH<sub>2</sub>O) or soot formation via acetylene (C<sub>2</sub>H<sub>2</sub>), identified by A2 rate of production. It was noted that oxidation was the preferred pathway for concentrations of toluene below 5 mol% of the fuel due to higher availability of OH and H from the reaction zone which promotes the oxidation [45, 48]. This effect is reported to change at larger concentrations, consequently it was suggested that doping and blending should be considered different regimes with respect to soot loading. It was concluded that toluene is a promising candidate for doping in hydrogen flames to improve the radiative heat transfer [45]. The efficacy of toluene in a binary n-heptane or iso-octane dopant mixture has also been considered previously, where a positive non-linear correlation between toluene-containing fuels and soot production is reported [49, 50]. Russo et al. [51] investigated the sooting effects of prevapourised toluene in premixed methane flames and found similarly that toluene doped flames yielded higher soot concentrations.

The potential for toluene as a fuel additive to improve thermal radiation has been well established in previous work but there is still a need for further investigation to assess its efficacy under more industry-representative conditions. The study by Evans et al. considered only simple jet flames with relatively low turbulence intensity [45]. Additionally, by only considering pure hydrogen blended with nitrogen, there was a penalty on flame temperature, and consequently, a strong effect on the overall reaction kinetics. Since the integration of hydrogen may happen gradually with low concentrations blended into current fuel blends, further investigation on the effects of blends of hydrogen in natural gas without inert diluents should be undertaken to build a more realistic picture. A significant novelty of this work is the study of toluene as a dopant in flames which are indicative of a transitional approach to hydrogen. That is, ensuring sufficient turbulence and recirculation to mimic industry combustors and considering realistic fuel blends including 10, 20 and 100 vol% hydrogen addition with specific reference to the properties of natural gas in the same burner system. This research combines experimental flame imaging techniques and heat flux data with computational modelling of soot precursors to report the efficacy of toluene as a soot surrogate for improving radiant heat transfer and visibility in turbulent hydrogen/natural gas flames stabilised on bluff-body burners to emulate the recirculation component of industry burners.

## 2 Methods

### 2.1 Experimental setup

The geometric complexities of full-scale industrial burners are difficult to replicate with lab-scale experiments, and likewise, characterisation of the governing chemistry and physics is challenging in large-scale systems. A common feature of industrial burner design is recirculation, most commonly achieved with modifications to the jet geometry or redirection of hot exhaust gases [52]. Recirculation, and its absence, can have a large effect on fuel/air mixing, residence time and overall stability [52, 53]. Bluff-body experimental burners were popularised by Masri et al. [54] and Dally et al. [55] and have since been used elsewhere in literature [53, 56-59] because they capture the key physics of recirculated flow in a controllable and characterisable way. A bluff-body burner creates recirculation and provides increased stability, which is useful in turbulent flames. The combustion conditions created by bluff-body burners are similar to practical combustors used in many industry applications. This geometry is therefore a useful tool in studying industry-representative flames while preserving relatively simple and well-defined boundary conditions [60]. It is due to their ability to emulate industry burner physics and help stabilise highly turbulent flames that bluff-body burners are used in this investigation.

In this investigation, the experimental results are collected using the burner apparatus presented in Figure 1 and described previously [33, 61]. The burner consists of a cylinder with a central 4.6-mm-diameter jet ( $d_{jet}$ ), from which the fuel is issued. Two burners with external diameters ( $d_{BB}$ ) of 50 mm and 64 mm are used. A 4.6 mm central jet is chosen as it is commonly used in literature [62, 63] and frequently used with these bluff-body diameters [33, 61]. The burner is positioned in the centre of a co-flowing air stream and raised 10 mm above the annular flow constrictor for visibility. Co-flowing air produces a recirculation of hot gases, allowing the flame to stabilise [60]. This design enables the control of recirculation by adjusting the jet and co-flow inlet conditions independently to simulate various operating conditions. An annular contractor with a diameter ( $d_c$ ) of 190-mm, with honeycomb mesh around the bluff-body burner, delivering uniform co-flow air to the flame. The co-flow velocity is maintained at 11 m/s and 20 m/s for the hydrogen and natural gas/hydrogen flames, respectively. It should be noted that the momentum flux ratio ( $\rho_{jet}U_{jet}:\rho_{coflow}U_{coflow}$ ) between these cases varies by no more than 8% across all cases. This ratio has been shown to be the dictating parameter for the vortical structure and the length of the recirculation zone [33, 55].

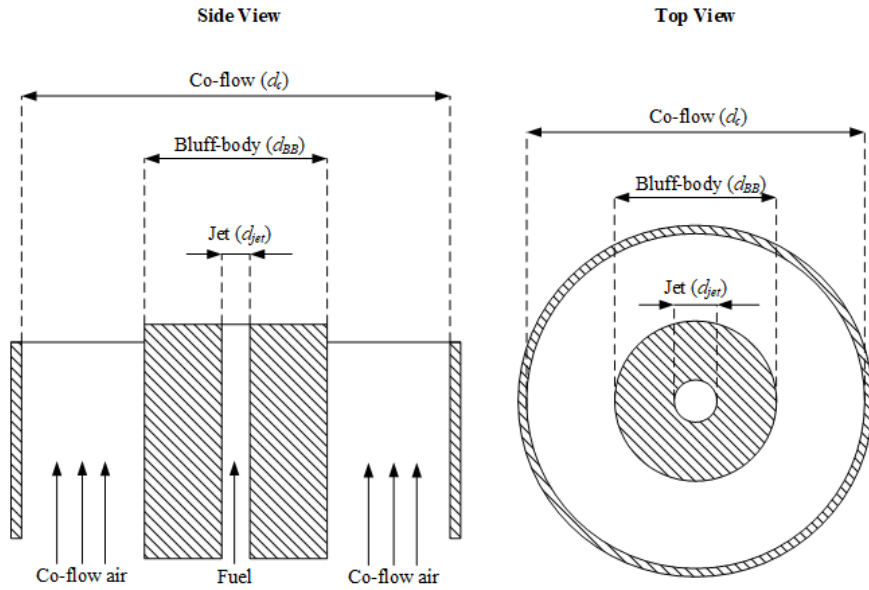


Figure 1: Diagram of the bluff-body burner and annular air contractor arrangement where  $d_{jet} = 4.6$  mm,  $d_{BB} = 50$  or 64 mm and  $d_c = 190$  mm

Liquid toluene (assay: 99.5%) is vapourised at 150°C using a Bronkhorst Controlled Evaporator and Mixer (CEM). Toluene, at 1–5 mol%, is added to 10, 20 and 100 vol% hydrogen (assay: 99.999%) in natural gas fuel blends. A bulk mean jet Reynolds number of 10,000 is kept constant for all cases to ensure sufficiently turbulent conditions. The gas density, viscosity and velocity used to calculate Reynolds number are recorded in Table S1 of the supplementary data, the characteristic length is chosen as  $d_{jet}$ . Gas mixture data is calculated using previously established methods [64]. Composition of natural gas is also presented in the supplementary material (Table S2).

The heat transfer properties of the flames are primarily characterised by data collected from heat flux sensors (Medtherm 92241/2), to compare the radiative properties of flames with different fractions of hydrogen. Thermocouples measuring the temperature differential between the sensor surface and an internal heat sink form an electromotive force at the output which is directly proportional to the heat transfer rate. A conversion factor calibrated to the specific sensor is used to convert the measured voltage to heat flux. Voltage samples are taken at a frequency of 1000Hz for 30 seconds and a mean value is presented for each flame with corresponding uncertainty derived from the average variance between samples. To compare the flame structure and visibility for different burners and fuel blends, a DSLR camera (Canon EOS 6D) with a 50 mm lens is used for the flame photographs. Imaging is through a 594-nm (23-nm full-width at half maximum) notch filter to eliminate the orange colour—this particular colour has been reported previously [65, 66] and attributed to sodium impurity corresponding to 589-nm, despite the use of high purity fuels. In this instance, the spectrometry data and comparison photos with and without the filter are used to highlight the presence of sodium. Flame photographs are helpful when presenting the effects on flame structure and colour, but can be misleading when discussing visibility and brightness to the naked eye due to any manipulation of the aperture and exposure times. A Lux meter (Protech QM1584) is used to measure flame brightness, or more specifically, flame illuminance (lumen/m<sup>2</sup>), to further characterise and quantify the visibility of the flame cases.

## 2.2 Computational analysis

Numerical simulations of opposed-flow diffusion (OPPDIF) flames in Chemkin Pro v19.2 are used in combination with the experimental data to describe the flame behaviour and underlying chemistry. An opposed-flow configuration is chosen because it enables the study of soot formation and oxidation under idealised flow fields, which, in turn, enables a focus on the chemistry effects. The OPPDIF model has been used previously to study flame phenomena in jet flame burners, including bluff-bodies [67, 68]. The OPPDIF model allows for analysis of homogeneous, gas-phase kinetics and sensitivity of a wide range of species or operating conditions. Sensitivity to the strain rate is considered, as it is an important parameter related to the burner design and operation, and affects the formation of species such as soot [69, 70]. Strain is defined as the velocity difference normalised to the axial distance between the fuel and the oxidant jets, 50 mm in this case. Variations in the strain rate are achieved by adjusting fuel and oxidant stream velocities, ensuring similar momentum, to position the stagnation plane in the middle of the domain. Gas velocities used in each case are summarised in Table S3 in the supplementary material.

A chemical mechanism developed by Cai and Pitsch [71] is used for modelling the PAH formation, up to and including pyrene (A4). The mechanism includes thermodynamic and transport data for 335 species and 1610 gas-phase reactions. The behaviour of soot precursors, namely naphthalene (A2), will be used as a predictor of overall soot production and corresponding thermal radiation. A2 is often used as a soot indicator species in numerical studies because it is the rate-limiting step in the formation of large PAHs [24, 45, 72]. Additionally, A2 is the closest PAH in size to toluene, focussing the analysis of the chemical pathways. Unless specified otherwise, A2 is described by the summation of individual A2-variant species, of which A2XC<sub>10</sub>H<sub>8</sub> is the dominant variant. Simulations of various H<sub>2</sub>/CH<sub>4</sub> fuel blends in air are considered across a range of strain rates to study the effects of different fuel blends under a variety of operating conditions.

### 3 Results and Discussion

#### 3.1 Flame photographs and illuminance

Turbulent flames of hydrogen and blended hydrogen/natural gas were stabilised on two bluff-body burners with different diameters, and prevapourised toluene was added to the fuel stream at 1–5 mol%. Photographs for the hydrogen flames and hydrogen/natural gas flames (with 10 vol% hydrogen) at various levels of toluene addition are presented in Figure 2 and Figure 3, respectively. For each combination of base fuel and level of toluene addition, the presented image is a composite of two photos, corresponding to the two bluff-body diameters, namely 64 mm and 50 mm-diameter on the left and right side of the centreline, respectively.

The general structure of all flames is comparable to other bluff-body flames seen in literature [33, 55, 58, 61, 73] with three distinct zones present for each flame case — an initial recirculation zone followed by a high-strain neck zone and finally the jet-like downstream region [74]. Blends at 10 and 20 vol% hydrogen in natural gas flames are very similar to the reference natural gas flame for both bluff-body diameters without the addition of toluene. In these cases, the addition of hydrogen to natural gas has no observable effect on flame structure or visibility, with the exception of the 50 mm burner, which became brighter with the addition of hydrogen. This is consistent with previous investigations highlighting hydrogen addition up to 20 vol% having a negligible effect on flame length or overall structure [13]. Where the effect of hydrogen compared to methane is investigated in the literature, this result builds on existing work which describes a similarly unremarkable effect on the velocity contour plots in bluff-body burners [57]. A stronger contrast is observed between the reference natural gas and 100 vol% hydrogen flame cases. In this case, the 100 vol% hydrogen flames' recirculation zones became longer than the pure natural gas, consistent with previous investigations [21]. A consequence of hydrogen addition is that as the hydrogen content in the fuel grows the stoichiometric mixture fraction decreases. A table of stoichiometric mixture fractions for all fuel blends is included in the supplementary material (Table S3). The stoichiometric mixture fraction for hydrogen is almost 50% lower than for natural gas. This causes the location of stoichiometric combustion, referred to as the stoichiometric contour line [75], to shrink inward towards the jet centreline. This contributes to the shorter and thinner flames in comparison to natural gas, as seen in Figure 2. The flames overall became shorter and were significantly less visible than the reference natural gas flames, with photographs for the 100 vol% hydrogen (0 mol% toluene) taken at double the exposure time and with an aperture allowing 12 times more light than that of the natural gas flame photographs—thus the image intensity of the hydrogen flame is 24 times less bright than the equivalent natural gas photograph. The reduction in flame length due to hydrogen addition is commonly reported in literature [11, 13, 14] however, the effects of toluene on flame height in bluff-body burners for these fuel blends has not previously been reported. The notch-filtered photographs of the 100 vol% hydrogen flames show a pale blue/red compared to the yellow of the natural gas flames and are otherwise invisible to the naked eye. Toluene addition causes a noticeable increase in brightness for the 10, 20 and 100 vol% hydrogen flames. These flames are brighter and begin to take on a yellow colour typical of sooting flames with increasing toluene concentrations, which is consistent with previous investigations of toluene addition to a hydrogen-based flame [45], however this work provides a new insight into the effect of toluene on visibility for blended and bluff-body stabilised hydrogen/natural gas flames — compared to previous literature which only considered simple jet hydrogen/nitrogen flames at a lower turbulence regime. Incremental increases in toluene concentration result in a visibly more luminous yellow flame, most notably in the recirculation and jet regions of the bluff-body flame. As toluene concentrations increased, the recirculation zone length increases while the high-strain neck zone length decreases. The flames also become fractionally taller and wider with increasing toluene concentration for the 100 vol% hydrogen fuel and, albeit to a lesser extent, the 10 or 20 vol% hydrogen flames. The trends observed for base fuel and toluene addition are seen consistently in both bluff-body diameters. Reducing the bluff-body diameter from 64 mm to 50 mm causes a visible reduction in the recirculation zone brightness, width and length, and a visible increase in the total flame length, consistent with previous investigations [21]. This is due to a smaller

recirculation zone in the 50 mm burner, allowing more fuel to be burnt further downstream [33]. Reducing the bluff-body diameter appears to reduce the visibility of the reference natural gas flame significantly, but this trend is not seen consistently for the fuels containing hydrogen.

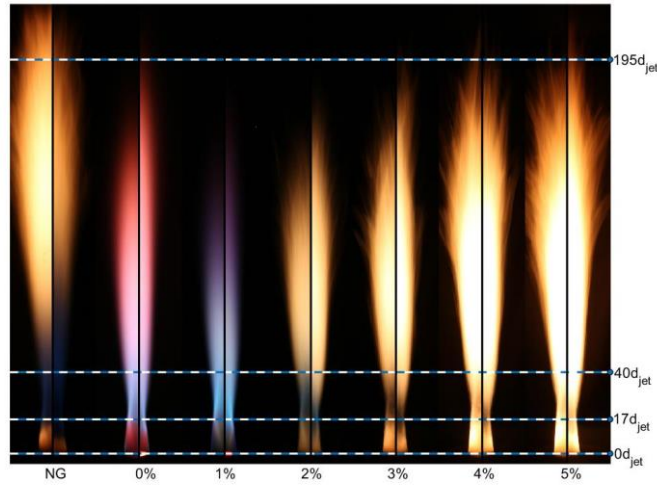


Figure 2: Split photographs natural gas flames with 100 vol% hydrogen, with the addition of 1-5 mol% toluene and stabilised on the 64 mm (left-half) and 50 mm (right-half) bluff-body burner. Reference natural gas (NG) flame photos also included. All flames are operated at  $Re = 10,000$ . Aperture and exposure settings from left to right:  $f/22$  2s,  $f/1.8$  4s,  $f/22$  30s, 2s,  $1/5s$ ,  $1/5s$ ,  $1/5s$ .

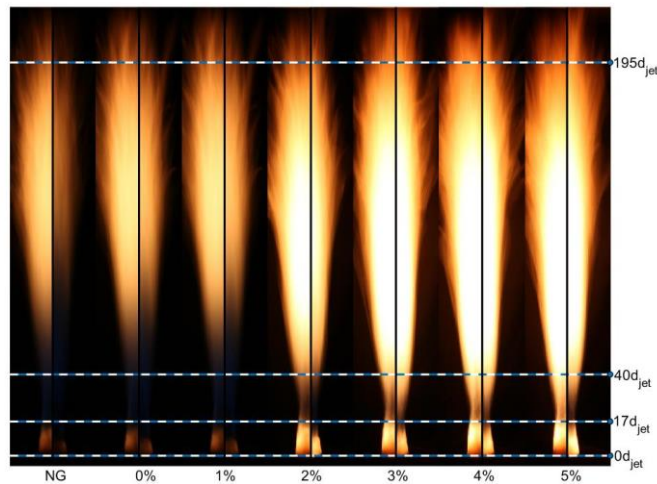


Figure 3: Split photographs of natural gas flames with 10 vol% hydrogen, with the addition of 1-5 mol% toluene and stabilised on the 64 mm (left-half) and 50 mm (right-half) bluff-body burner. Reference natural gas (NG) flame photos also included. All flames are operated at  $Re = 10,000$ . Aperture and exposure settings from left to right:  $f/22$  1s, 1s,  $1/2s$ ,  $1/2s$ ,  $1/2s$ ,  $1/2s$ ,  $1/2s$ .

Figure 4 presents the flame illuminance data as a supplement to flame photographs (Figure 2 and Figure 3). Illuminance measurements are a way of capturing and quantifying the brightness in a way that enables a direct comparison of flame photographs with the heat flux measurements. The illuminance data supports the trends implied from the photographs, with illuminance increasing for each level of toluene addition. It is noteworthy that 2–3 mol% toluene is required for the pure hydrogen flames to emit equivalent illuminance to that of the natural gas reference case, as shown in Figure 4. This is significant due to the safety concerns regarding the low visibility of hydrogen and flame detection [27]. The blended hydrogen/natural gas flame cases, with both 10 and 20 vol% hydrogen, exhibit a similar increase in illuminance with toluene addition. The flame illuminance in Figure 4 does not decrease



notably from that of pure natural gas for the addition of 20 vol% hydrogen (without toluene). This suggests that for natural gas fuel blends containing up to 20 vol% hydrogen, toluene is not required to improve flame illuminance. Previous investigations have shown a similarly unremarkable effect of hydrogen addition up to 20 vol% in hydrocarbon flames concerning reduced visibility [13, 76] — however, quantification of the effect of hydrogen addition to natural gas with respect to toluene addition to improve visibility via soot loading is a novel contribution of this paper. The differences between 10 and 20 vol% hydrogen are also minor. Comparing both bluff-body diameters, a similar trend is observed with no significant effects on flame visibility between the 50 mm and 64 mm burners; apart from the natural gas reference cases, where the 64 mm burner is notably brighter than the 50 mm. It is interesting to note, however, that this trend is not observed for the pure and blended hydrogen cases. The discrepancy between cases with and without hydrogen is most likely the result of competing factors extending the residence time. In the 64 mm-bluff-body case, the flame has a recirculation zone that is larger than that observed in the 50 mm-bluff-body case, which helps promote the soot formation with its relatively long residence time. In contrast, the 50 mm-bluff-body flame has a longer flame length, which indicates a longer global residence time than the 64 mm-bluff-body flame. The proximity of the data points makes conjectures about the trends between burners difficult but, nevertheless, they can be used to supplement visual observations and trends in the heat flux data and soot precursor concentrations.

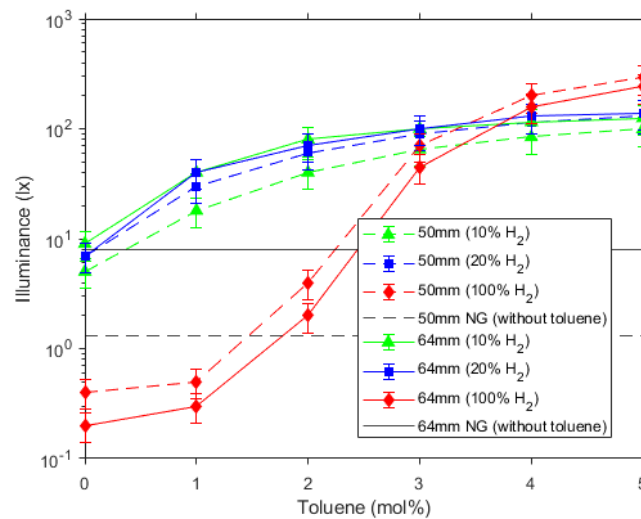


Figure 4: Illuminance (lx) measurements of turbulent pure and blended H<sub>2</sub> in natural gas (NG) (vol%) for the addition of 1-5 mol% toluene, and reference natural gas cases (without toluene addition) in a 50 mm and 64 mm bluff-body burner.

### 3.2 Flame heat flux

Thermal radiation heat flux measurements for all flames are presented in Figure 5 and Figure 6, for the 64 mm and 50 mm bluff-bodies, respectively. The heat flux data is normalised by the heat input from the fuel. It is logical that since both flame heat flux and flame illuminance are strongly dependant on toluene or soot concentration that a correlation may be seen in the two data sets. Figure S2 in the supplementary material combines Figure 4 and Figure 5 to highlight the shared dependence on toluene concentration and resulting soot formation. In bluff-body flames soot accumulation and oxidation can be considered in the three distinct zones of a bluff-body flame, consequently changes to the characteristics of these zones affects how soot is produced and oxidised within them. Previous work by Rowhani et al. [61] has shown that in bluff-body flames soot volume fraction peaks first in the recirculation zone and in the downstream jet-like region, with almost no soot being produced in the neck zone due to high strain rates. It was also shown that the soot accumulation in the recirculation zone almost doubles by increasing the bluff-body diameter from 38mm to 50 mm and then to 64 mm while the neck zone remains fairly consistent. Soot accumulation in the downstream region tends to increase

with decreasing bluff-body diameter since this reduces the recirculation zone size and intensity allowing for more fuel to be burnt downstream. It has been previously established that decreasing the fuel to air ratio, perhaps by increased recirculation of air, also leads to reduced accumulation of soot in a recirculation due to increased oxidation [77]. Data in Figure 4, Figure 5 and Figure 6 shows evidence of this via a larger total illuminance and heat flux, respectively, in the 50 mm bluff-body compared with the 64 mm. This suggests a larger content of fuel being burnt downstream and less being accumulated and burnt in the recirculation zone.

The normalised heat flux increases with increasing toluene concentration in all cases. The trends in the heat flux data are similar to that of illuminance, with the exception of the natural gas cases. The illuminance for natural gas in the 64 mm burner is almost 10 times greater than in the 50 mm burner. A discrepancy this large is not observed in the heat flux data. Additionally, a 10 vol% hydrogen blend (without toluene) significantly improves flame illuminance compared with the natural gas case in the 50 mm bluff-body. Otherwise, no significant reduction in heat flux is recorded for hydrogen addition of 10-20 vol% in natural gas, and thus, the addition of toluene does not appear to be required for these concentrations; however, the heat flux can be significantly improved by the addition of toluene. The pure hydrogen flame heat flux is approximately 80% lower than the pure natural gas case. To account for this reduction, a dopant concentration of 4 mol% toluene is required for the heat flux of the pure hydrogen flames to be equivalent to a natural gas flame. It should be noted that for toluene, the addition of 4 mol% in a pure hydrogen flame equates to 65% by mass, and 38% by energy input. This significant contribution of mass and enthalpy from the dopant is a limitation of the use of toluene as a means of supplementing reduced radiative heat transfer in hydrogen flames. This is most likely the cause of the more significant effects of toluene on flame structure and visibility in the pure cases compared with the blended cases, since its contribution to enthalpy and mass by toluene becomes much greater in the 100 vol% hydrogen cases as a result of the increased volumetric flow to maintain a Reynolds number of 10,000.

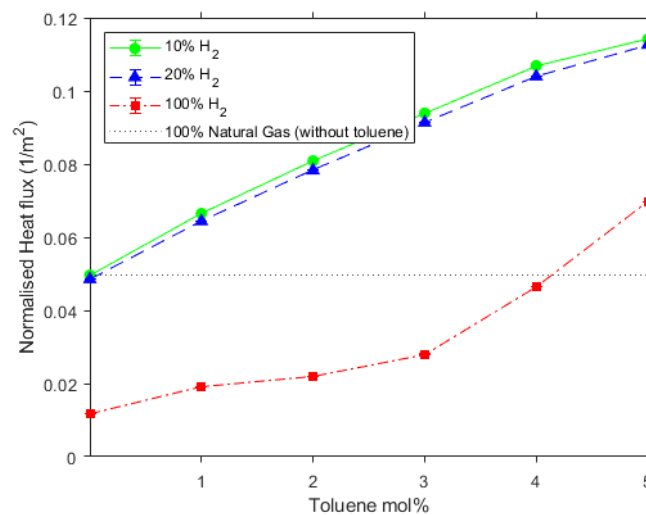


Figure 5: Heat flux data (normalised by heat input) for addition of 1–5 mol% toluene to pure and blended hydrogen/natural gas turbulent flames in a 64 mm bluff-body burner.

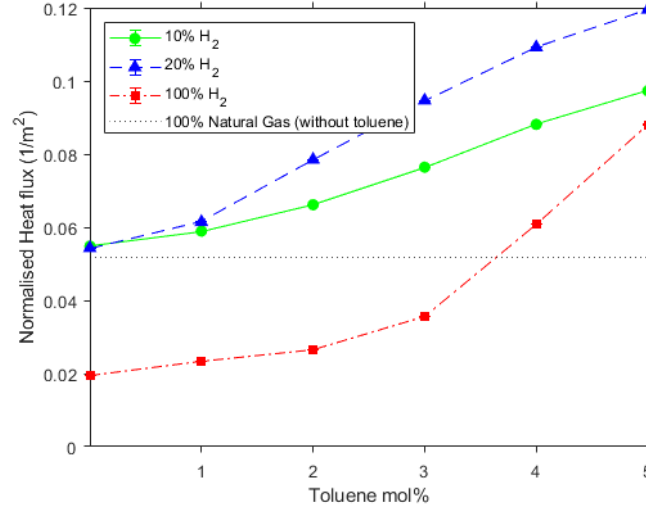


Figure 6: Heat flux data (normalised by heat input) for addition of 1–5 mol% toluene to pure and blended hydrogen/natural gas turbulent flames in a 50 mm bluff-body burner.

### 3.3 Computational analysis

To validate that the measured variations in heat flux are a consequence of increased soot formation due to toluene addition, the contribution of temperature and other radiant gases such as CO<sub>2</sub> and H<sub>2</sub>O are considered. An approach adapted from previous work [78, 79] using numerical data from an OPPDIF simulation of the aforementioned flame cases at two different strain rates are presented in Figure 7. Here it can be seen that toluene addition has a negligible effect on flame temperature. In this case, radiative heat losses are a function of the temperature, soot volume fraction and an absorption coefficient (the Planck mean) [78, 79]. The variation in temperature with respect to toluene addition, as shown in Figure 7, is not only too small to cause the experimentally measured variation in heat flux, since a 25K peak temperature variation would only result in a 13% change in radiant losses – but toluene addition has a reducing effect on the peak flame temperature. The experimentally measured variation in heat flux is much greater than this and therefore, given the contribution to the radiant heat loss from the soot volume fraction is much greater than the absorption coefficient, it can be assumed that the large variations in the experimental heat flux are primarily a consequence of increased soot loading due to toluene addition.

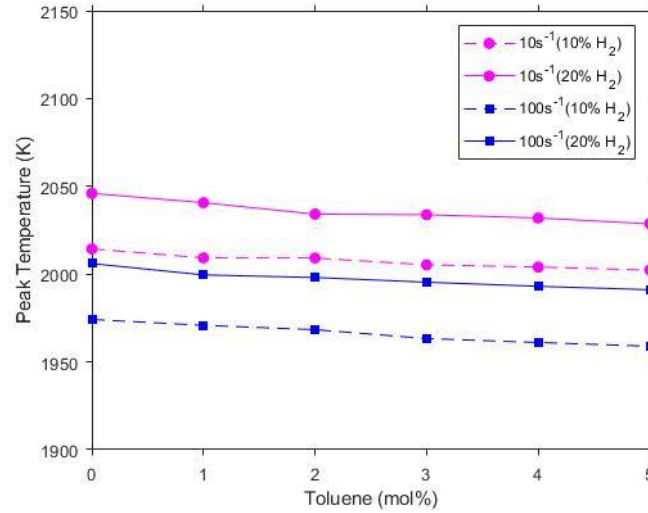


Figure 7: Calculated peak flame temperature from opposed-flow simulations with H<sub>2</sub>/CH<sub>4</sub> fuel blends, doped with 1-5 mol% toluene at two different strain rates.

Comparing the heat flux trends in Figure 5 and Figure 6, that is, between the bluff-body diameters, it can be seen that both bluff-body diameters broadly exhibit similar trends. The 50 mm bluff-body diameter yields a consistently higher normalised heat flux than the 64 mm bluff-body diameter for toluene addition to the pure hydrogen fuel, whereas the 64 mm bluff-body burner produces a higher heat flux for toluene addition to the 10 vol% hydrogen-natural gas blend. Assuming changes in the soot volume fraction are the primary cause for variations in the normalised heat flux, then a link may be established between bluff-body diameter, and its effect on flame structure and resulting particle residence time and soot formation.

Typically, increased recirculation results in increased residence time, which promotes soot formation [53, 80, 81]. It has been reported previously that increasing the bluff-body diameter from 38-mm to 50 mm and 64 mm can double the recirculation zone length leading to increased particle residence time, which can increase the amount of soot formation [53]. It is also noteworthy that flame images presented in this paper show that a reduced bluff-body diameter causes a subsequent reduction in recirculation zone size but an increase in overall flame length by as much as 22% in some cases. This would also extend particle residence time and promote increased soot formation. This is also supported in literature with similar investigations of soot in bluff-body burners reporting a global decrease in the soot volume fraction of flames despite seeing local increases in regions of high recirculation [33]. Experimental data presented in Figure 5 and Figure 6 both show evidence of increased residence time via a combination of increased flame length and increased recirculation zone size. Comparison of visual luminosity of flame images (Figure 2 and Figure 3) provides an insight into local soot behaviour, where a more luminous region suggests a higher concentration of soot. For example, toluene addition to the pure hydrogen flames in the 50 mm bluff-body burner appear consistently brighter in their downstream region compared to the 64 mm burner (Figure 2). This observation is also reflected in the illuminance data (Figure 4). Similarly, the more luminous recirculation zones up to twice the length in the 64 mm burner compared with the 50 mm burner suggests a higher concentration of soot within the recirculation zone. It is also important to mention the effects of differential diffusion on soot formation, shown previously to be an important factor in the formation of soot as it relates to species' transport phenomena, especially for fuel mixtures containing hydrogen, which is highly diffusive [82, 83]. The impact of hydrogen addition, and subsequent change in differential diffusivity, have been previously reported to affect factors such as flame length [84]—which, as mentioned previously, can affect residence time and soot formation.

Another noteworthy observation is the shape of the curves in Figure 5 and Figure 6 for the blended hydrogen/natural gas cases in the 50 mm burner compared with the 64 mm burner. The 64 mm data plotted in Figure 5 follow a consistent curve for both the 10 and 20 vol% hydrogen cases, with the 10 vol% hydrogen resulting in slightly higher heat flux at each increment of toluene addition. However, this trend is not seen in the 50 mm data presented in Figure 6. Here, the data diverges as the toluene concentration increases, and, perhaps most interestingly, the 20 vol% hydrogen cases result in a higher heat flux compared to the 10 vol%. It is not appropriate to assume that, because heat flux measurements were normalised to thermal input, this is not a consequence of increased flame temperature, since radiation does not respond linearly with temperature ( $Q_{\text{rad}} \propto T^4$ ). However, given the discrepancy is between burners and not fuel mixtures, and since the fuel blends for both burners are the same, this is unlikely to be a consequence of increased temperature due to hydrogen addition. Thermal and chemical-promoting effects of soot are well documented for the addition of hydrogen to a hydrocarbon mixture compared with an inert diluent [29-31, 85] with various explanations given as to why. It is worth noting that to preserve Reynolds number in flames with varying compositions of fuels each with significantly different densities, jet velocity cannot be conserved between cases. This means for cases with relatively higher jet exit velocities, an increase in the fuel to air co-flow momentum flux ratio entrains less fuel into the recirculation zone near the bluff body surface. This leaner recirculation zone, in combination with a reduced residence time may result in an inhibition of soot nucleation and surface growth while soot oxidation is promoted. This effect was shown previously for bluff-body stabilised ethylene/hydrogen flames by Deng et al. [74] where a leaner recirculation zone inhibited soot formation due to changes in jet velocity. This may explain the discrepancy between bluff-body diameters (Figure 5 and Figure 6) where the 20 vol% hydrogen fraction increases the fuel to air momentum flux ratio compared to the 10 vol% mixture, allowing for a leaner recirculation zone and a more dispersed soot concentration. This may not have occurred in the 64mm bluff-body diameter due to a stronger recirculation zone compared to the 50mm.

An alternative or additional cause may be increased strain rate in the 50 mm burner compared with the 64 mm. Reducing the bluff-body diameter and resulting recirculation zone size will increase the strain rate at the jet exit [33, 86, 87]. Too high a strain rate will restrict the combustion and push the system closer to its extinction strain rate [86, 87]. A fuel mixture with a much higher extinction strain rate, such as one with a higher hydrogen content [88], may allow for more soot formation than a less resilient mixture through increased reactivity. Numerical simulations of an OPPDIF flame are used to test this hypothesis and examine the effects of the strain rate more closely. An OPPDIF model considers a one-dimensional (1D) flame created using opposed-flow fuel and oxidant streams. This 1D flame is representative of a local flame-front embedded within the larger, more complex bluff-body flame. In practice, these 1D flames encompass the flame and strain rate as a product of interactions between the fuel and the air streams. In this way, the governing reaction kinetics can be studied without the need to consider turbulent chemistry interactions, which are computationally more demanding and can be difficult to isolate in terms of specific variables. In this instance, the base fuel blends and toluene concentrations have been considered in the OPPDIF model for different strain rates.

The numerical modelling of the soot precursors in the flame cases in an OPPDIF configuration considered in this paper appear to support the hypothesis that increases in strain rate from a reduction in the bluff-body diameter caused the larger hydrogen blend to yield a higher heat flux. In the supplementary material provided, Figure S1 shows the relationship between A2 rate of production (ROP) and the strain rate as a function of the axial distance. It can be seen that the peak A2 formation primarily occurs for low strain regions of the flame. The inverse relationship between soot formation and strain rate has been seen previously in literature [24, 89]. In particular this has been shown for instantaneous soot volume fraction measurements in bluff-body flames [61]. This work further contributes to this well-established relationship by considering it with respect to soot precursors descended from toluene doped into hydrogen/natural gas flames. The numerical results presented in Figure 8 show the effect of the strain rate on the fuel mixtures considered in the experimental cases. A

similar trend to the experimental data is observed, where at higher strain rates the fuel blend with more hydrogen results in a higher A2 ROP. In this case, the distinction between 10 and 20 vol% hydrogen is very minor but a consistent trend is observed, nevertheless.

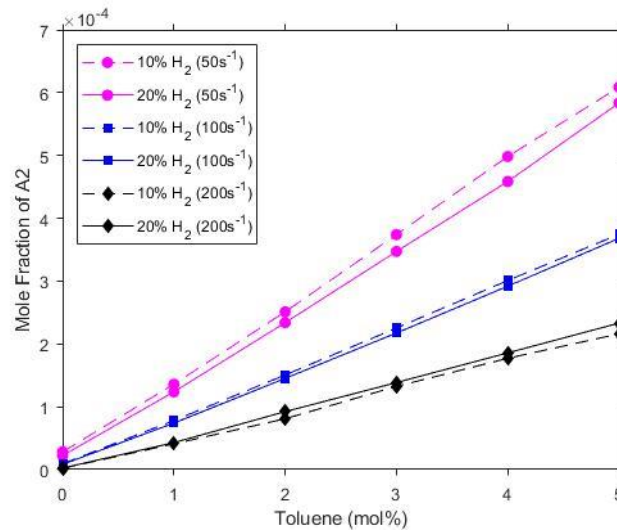


Figure 8: Calculated A2 mole fraction from opposed-flow simulations with H<sub>2</sub>/CH<sub>4</sub> fuel blends, doped with 1-5 mol% toluene at three different strain rates.

An analysis of chemical reaction pathways shows two main pathways are possible: either oxidation via formaldehyde (CH<sub>2</sub>O) or soot formation via acetylene (C<sub>2</sub>H<sub>2</sub>). The strain rate has the strongest influence on reaction pathway preferences. The reaction pathway diagrams are given for a 5 mol% toluene addition to 10 vol% hydrogen at strain rates of 10 s<sup>-1</sup> and 200 s<sup>-1</sup> in Figure 9 and Figure 10, respectively. The effect of the hydrogen content (up to 20 vol%) and toluene addition (up to 5 mol%) did not significantly affect the reaction pathways when compared with the strain rate. While the toluene addition did not significantly impact the chemical pathways, its presence does shift the reaction away from the oxidative pathway and towards the formation of A2 and, subsequently, soot. Previous investigations have noted the competing formation of soot via A2 and oxidation via formaldehyde [45]. The effect of toluene on the ROP ratio between formaldehyde and A2 is presented in Figure 11. A similar trend is seen here where at low toluene concentrations (<1 mol%) the oxidative tendencies of a hydrogen flame create a large discrepancy between the 10 and 20 vol% fuel blends—but as toluene concentration increases these become negligible.

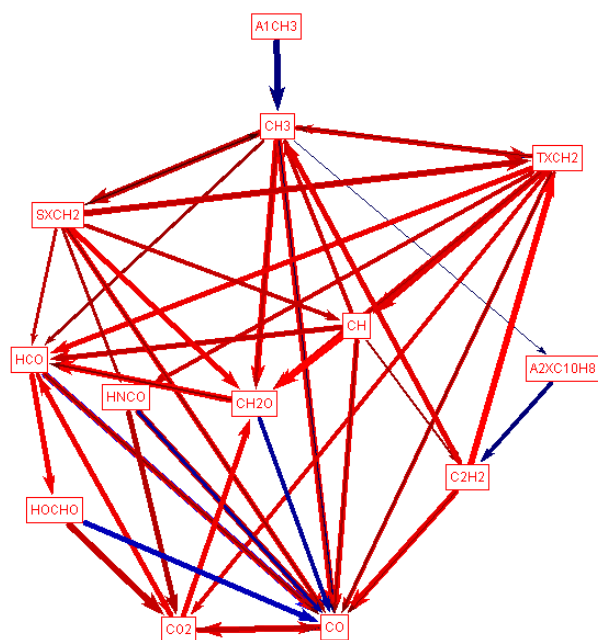


Figure 9: Reaction pathway diagram for toluene ( $A1CH_3$ ) conversion to  $A2XC_{10}H_8$  for 5 mol% toluene to a 10 vol% hydrogen in a methane fuel mixture at a strain rate of  $10\text{ s}^{-1}$ . Line thickness and colour correspond to the relative rates of production and exo- (red)/endo (blue)-thermic reactions, respectively.

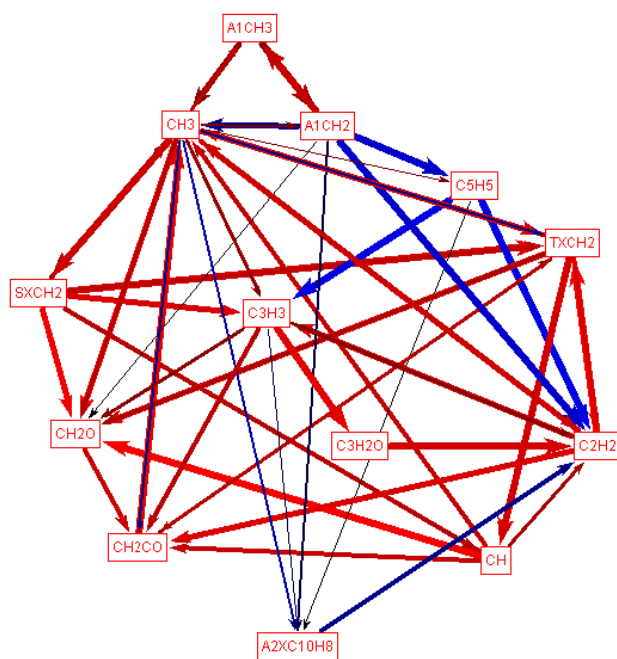


Figure 10: Reaction pathway diagram for toluene ( $A1CH_3$ ) conversion to  $A2XC_{10}H_8$  for 5 mol% toluene to a 10 vol% hydrogen in a methane fuel mixture at a strain rate of  $200\text{ s}^{-1}$ . Line thickness and colour correspond to the relative rates of production and exo- (red)/endo (blue)-thermic reactions, respectively.

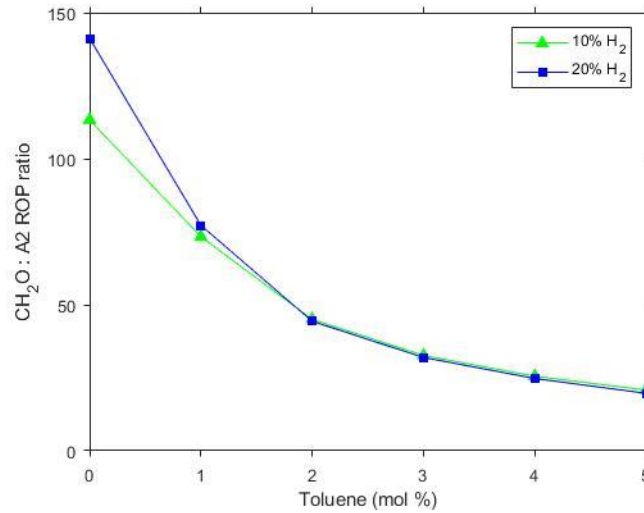


Figure 11: Calculated ROP ratio between formaldehyde (CH<sub>2</sub>O) and naphthalene (A<sub>2</sub>) in opposed-flow fuel/air simulation for toluene addition to a 10 and 20 vol% H<sub>2</sub> in a CH<sub>4</sub> flame with a strain rate of 10 s<sup>-1</sup>.

Figure 12 considers these strain rates at a wider selection of hydrogen concentrations to examine how this phenomenon behaves as the hydrogen content increases beyond 20 vol%. As the hydrogen concentration increases to 50 vol%, the effects of the strain rate become negligible with respect to A<sub>2</sub> ROP, as this tends to zero when the hydrogen fraction approaches 100 vol%. As expected, based on the experimental data and trends in Figure 8, at strain rates close to the extinction limit, the negative effects of hydrogen blending with A<sub>2</sub> ROP are lessened, with an apparent improvement seen of up to 20 vol% hydrogen for the 200 s<sup>-1</sup> case. This implicates that more hydrogen results in less soot and/or radiation may not apply to every burner, mode of operation or even every region within a flame.

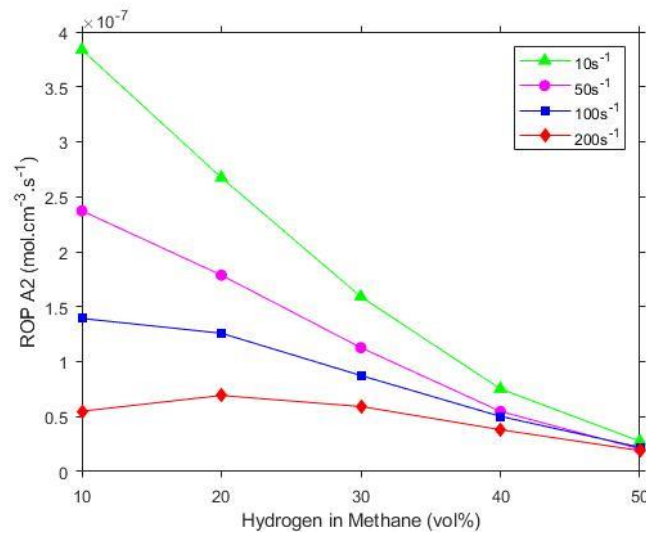


Figure 12: Calculated A<sub>2</sub> rate of production (ROP) in opposed-flow simulations with H<sub>2</sub>/CH<sub>4</sub> fuel blends at different strain rates.

It is worth noting that previous work by Evans et al. [45] reported a preference for oxidation (as opposed to soot formation) for concentrations of toluene < 5 mol%. This was linked to a higher availability of OH and H species but no data was presented which compares the effect of strain rate or residence time. A change in strain rate has also been shown to affect these species [90]. The implication from the data presented in this paper that strain rate is a key parameter with regard to soot formation in the presence of hydrogen/natural gas flames is an important addition to the knowledge contributed by Evans et al [45].



## 4 Conclusions

The efficacy of toluene addition to pure and blended hydrogen/natural gas flames on soot formation and the resulting radiative heat transfer, flame visibility and structure have been studied using a combination of experimental and computation methods. The experimental cases consisted of a series of turbulent diffusion flames stabilised on a 50 mm and a 64 mm bluff-body burner, while the computational work was simulated in an opposed-flow diffusion flame model at various strain rates. This work builds on previous investigations regarding the use of toluene as a dopant by assessing its efficacy on highly turbulent pure and blended hydrogen/natural gas flames stabilised on bluff-body burners.

1. Supplementing flames containing hydrogen with prevapourised toluene improves the colour, illuminance and overall visibility of bluff-body stabilised flames- both for pure hydrogen flames and blended hydrogen/natural gas flames. Approximately 2 mol% toluene is required in the pure hydrogen flames to achieve the equivalent illuminance of a natural gas flame.
2. Toluene addition has a positive effect on the normalised heat flux data in both bluff-body burners. Hydrogen addition up to 20 vol% does not have a measurable impact on the normalised heat flux, while a complete substitution of natural gas for hydrogen results in an 80% reduction in the normalised heat flux. Approximately 4 mol% toluene is required to bring the pure hydrogen flames output equal to that of a pure natural gas flame. In this case, however, the significant contribution of mass and enthalpy from the dopant is a limitation on the use of toluene as a means of supplementing the reduced radiative heat transfer in hydrogen flames. This is a significant contribution to previous work which did not consider toluene's efficacy with respect to pure natural gas and its limitations for use as a dopant in large quantities.
3. Reducing the bluff-body diameter has a notable effect on the outcomes of hydrogen addition. In the smaller 50 mm bluff-body burner, hydrogen addition of 20 vol% resulted in a higher normalised heat flux than the 10 vol% cases, while the opposite effect was observed in the larger 64 mm bluff-body. This suggests that not only may the negative effects of hydrogen addition on thermal radiation be negated under some conditions, but that hydrogen addition may be beneficial to radiation.
4. The findings from the fuel/air OPPDIF simulations show a strong improvement in soot precursor rates of production via the acetylene pathway with the addition of toluene. The impact of hydrogen addition is strongly dependent on operating strain rate but it should be noted that hydrogen addition is negligible, if not mildly beneficial up to 20 vol% at high strain rates to soot precursor production.

## 5 Declaration of Competing Interest

None.

## 6 Acknowledgements

The authors would like to acknowledge the support from The Australian Research Council, The University of Adelaide and the Future Fuels CRC (RP1.4-03). The authors also thank Douglas Proud for his assistance with this work.

## References

- [1]. Dreizler, A., Pitsch, H., Scherer, V., Schulz, C., and Janicka, J., *The role of combustion science and technology in low and zero impact energy transformation processes*. Applications in Energy and Combustion Science, 2021. **7**: p. 100040, DOI: <https://doi.org/10.1016/j.jaecs.2021.100040>.
- [2]. Pangborn, J., Scott, M., and Sharer, J., *Technical prospects for commercial and residential distribution and utilization of hydrogen*. International Journal of Hydrogen Energy, 1977. **2**(4): p. 431-445, DOI: [https://doi.org/10.1016/0360-3199\(77\)90050-7](https://doi.org/10.1016/0360-3199(77)90050-7).
- [3]. Scott, M. and Powells, G., *Sensing hydrogen transitions in homes through social practices: Cooking, heating, and the decomposition of demand*. International Journal of Hydrogen Energy, 2020. **45**(7): p. 3870-3882, DOI: <https://doi.org/10.1016/j.ijhydene.2019.12.025>.
- [4]. Connolly, D., Lund, H., Mathiesen, B.V., and Leahy, M., *The first step towards a 100% renewable energy-system for Ireland*. Applied Energy, 2011. **88**(2): p. 502-507, DOI: <https://doi.org/10.1016/j.apenergy.2010.03.006>.
- [5]. Yilmaz, İ., Ratner, A., Ilbas, M., and Huang, Y., *Experimental investigation of thermoacoustic coupling using blended hydrogen–methane fuels in a low swirl burner*. International Journal of Hydrogen Energy, 2010. **35**(1): p. 329-336, DOI: <https://doi.org/10.1016/j.ijhydene.2009.10.018>.
- [6]. Emadi, M., Karkow, D., Salameh, T., Gohil, A., and Ratner, A., *Flame structure changes resulting from hydrogen-enrichment and pressurization for low-swirl premixed methane–air flames*. International journal of hydrogen energy, 2012. **37**(13): p. 10397-10404, DOI: <https://doi.org/10.1016/j.ijhydene.2012.04.017>.
- [7]. *Australia's National Hydrogen Strategy*, in Council of Australian Governments (COAG) Energy Council. 2019, Department of Industry, Science and Energy Resources: Canberra.
- [8]. Weber, R. and Mancini, M., *On scaling and mathematical modelling of large scale industrial flames*. Journal of the Energy Institute, 2020. **93**(1): p. 43-51, DOI: <https://doi.org/10.1016/j.joei.2019.04.010>.
- [9]. Dong, X., Nathan, G.J., Mahmoud, S., Ashman, P.J., Gu, D., and Dally, B.B., *Global characteristics of non-premixed jet flames of hydrogen–hydrocarbon blended fuels*. Combustion and Flame, 2015. **162**(4): p. 1326-1335, DOI: <https://doi.org/10.1016/j.combustflame.2014.11.001>.
- [10]. Kalbhor, A. and van Oijen, J., *Effects of hydrogen enrichment and water vapour dilution on soot formation in laminar ethylene counterflow flames*. International Journal of Hydrogen Energy, 2020. **45**(43): p. 23653-23673, DOI: <https://doi.org/10.1016/j.ijhydene.2020.06.183>.
- [11]. Choudhuri, A.R. and Gollahalli, S.R., *Combustion characteristics of hydrogen–hydrocarbon hybrid fuels*. International Journal of Hydrogen Energy, 2000. **25**(5): p. 451-462, DOI: [https://doi.org/10.1016/S0360-3199\(99\)00027-0](https://doi.org/10.1016/S0360-3199(99)00027-0).
- [12]. Wu, L., Kobayashi, N., Li, Z., Huang, H., and Li, J., *Emission and heat transfer characteristics of methane–hydrogen hybrid fuel laminar diffusion flame*. International Journal of Hydrogen Energy, 2015. **40**(30): p. 9579-9589, DOI: <https://doi.org/10.1016/j.ijhydene.2015.05.096>.
- [13]. Kumar, P. and Mishra, D.P., *Experimental investigation of laminar LPG–H<sub>2</sub> jet diffusion flame*. International Journal of Hydrogen Energy, 2008. **33**(1): p. 225-231, DOI: <https://doi.org/10.1016/j.ijhydene.2007.09.023>.
- [14]. Choudhuri, A.R. and Gollahalli, S.R., *Characteristics of hydrogen–hydrocarbon composite fuel turbulent jet flames*. International Journal of Hydrogen Energy, 2003. **28**(4): p. 445-454, DOI: [https://doi.org/10.1016/S0360-3199\(02\)00063-0](https://doi.org/10.1016/S0360-3199(02)00063-0).
- [15]. Gondal, I.A. and Sahir, M.H., *Prospects of natural gas pipeline infrastructure in hydrogen transportation*. International journal of energy research, 2012. **36**(15): p. 1338-1345, DOI: <https://doi.org/10.1002/er.1915>.
- [16]. Sen, S. and Puri, I., *Thermal radiation modeling in flames and fires*. Transport Phenomena in Fires, 2008: p. 301.

- [17]. Pessoa-Filho, J.B., *Thermal radiation in combustion systems*. Journal of the Brazilian Society of Mechanical Sciences, 1999. **21**(3): p. 537-547.
- [18]. Hamadi, M.B., Vervisch, P., and Coppalle, A., *Radiation properties of soot from premixed flat flame*. Combustion and Flame, 1987. **68**(1): p. 57-67, DOI: [https://doi.org/10.1016/0010-2180\(87\)90065-4](https://doi.org/10.1016/0010-2180(87)90065-4).
- [19]. Hutny, W.P. and Lee, G.K., *Improved radiative heat transfer from hydrogen flames*. International Journal of Hydrogen Energy, 1991. **16**(1): p. 47-53, DOI: [https://doi.org/10.1016/0360-3199\(91\)90059-R](https://doi.org/10.1016/0360-3199(91)90059-R).
- [20]. Brookes, S.J. and Moss, J.B., *Predictions of soot and thermal radiation properties in confined turbulent jet diffusion flames*. Combustion and Flame, 1999. **116**(4): p. 486-503, DOI: [https://doi.org/10.1016/S0010-2180\(98\)00056-X](https://doi.org/10.1016/S0010-2180(98)00056-X).
- [21]. Kashir, B., Tabejamaat, S., and Jalalati, N., *The impact of hydrogen enrichment and bluff-body lip thickness on characteristics of blended propane/hydrogen bluff-body stabilized turbulent diffusion flames*. Energy Conversion and Management, 2015. **103**: p. 1-13, DOI: <https://doi.org/10.1016/j.enconman.2015.06.028>.
- [22]. Hottel, H.C. and Sarofim, A.F., *Radiative transfer*. 1967: McGraw-Hill.
- [23]. Viskanta, R. and Mengüç, M.P., *Radiation heat transfer in combustion systems*. Progress in Energy and Combustion Science, 1987. **13**(2): p. 97-160, DOI: [https://doi.org/10.1016/0360-1285\(87\)90008-6](https://doi.org/10.1016/0360-1285(87)90008-6).
- [24]. Bisetti, F., Blanquart, G., Mueller, M.E., and Pitsch, H., *On the formation and early evolution of soot in turbulent nonpremixed flames*. Combustion and Flame, 2012. **159**(1): p. 317-335, DOI: <https://doi.org/10.1016/j.combustflame.2011.05.021>.
- [25]. Saito, K., Williams, F.A., and Gordon, A.S., *Effects of Oxygen on Soot Formation in Methane Diffusion Flames*. Combustion Science and Technology, 1986. **47**(3-4): p. 117-138, DOI: <https://doi.org/10.1080/00102208608923869>.
- [26]. Schiro, F., Stoppato, A., and Benato, A., *Modelling and analyzing the impact of hydrogen enriched natural gas on domestic gas boilers in a decarbonization perspective*. Carbon Resources Conversion, 2020. **3**: p. 122-129, DOI: <https://doi.org/10.1016/j.crcon.2020.08.001>.
- [27]. Hord, J., *Is hydrogen a safe fuel?* International Journal of Hydrogen Energy, 1978. **3**(2): p. 157-176, DOI: [https://doi.org/10.1016/0360-3199\(78\)90016-2](https://doi.org/10.1016/0360-3199(78)90016-2).
- [28]. Liu, F., Liu, Z., Sang, Z., He, X., Liu, F., Liu, C., and Xu, Y., *Kinetic study of the effects of hydrogen blending to toluene reference fuel (TRF)/air mixtures on laminar burning velocity and flame structure*. Fuel, 2020. **274**: p. 117850, DOI: <https://doi.org/10.1016/j.fuel.2020.117850>.
- [29]. Liu, F., Ai, Y., and Kong, W., *Effect of hydrogen and helium addition to fuel on soot formation in an axisymmetric coflow laminar methane/air diffusion flame*. International Journal of Hydrogen Energy, 2014. **39**(8): p. 3936-3946, DOI: <https://doi.org/10.1016/j.ijhydene.2013.12.151>.
- [30]. Wang, Y., Gu, M., Chao, L., Wu, J., Lin, Y., and Huang, X., *Different chemical effect of hydrogen addition on soot formation in laminar coflow methane and ethylene diffusion flames*. International Journal of Hydrogen Energy, 2021, DOI: <https://doi.org/10.1016/j.ijhydene.2021.02.014>.
- [31]. Boyette, W.R., Steinmetz, S.A., Guiberti, T.F., Dunn, M.J., Roberts, W.L., and Masri, A.R., *Soot formation in turbulent flames of ethylene/hydrogen/ammonia*. Combustion and Flame, 2021. **226**: p. 315-324, DOI: <https://doi.org/10.1016/j.combustflame.2020.12.019>.
- [32]. Xu, L., Yan, F., Wang, Y., and Chung, S.H., *Chemical effects of hydrogen addition on soot formation in counterflow diffusion flames: Dependence on fuel type and oxidizer composition*. Combustion and flame, 2020. **213**: p. 14-25, DOI: <https://doi.org/10.1016/j.combustflame.2019.11.011>.
- [33]. Rowhani, A., Sun, Z.W., Medwell, P.R., Alwahabi, Z.T., Nathan, G.J., and Dally, B.B., *Effects of the Bluff-Body Diameter on the Flow-Field Characteristics of Non-Premixed Turbulent Highly-*

- Sooting Flames*. Combustion Science and Technology, 2019: p. 1-19, DOI: <https://doi.org/10.1080/00102202.2019.1680508>.
- [34]. Wu, L., Kobayashi, N., Li, Z., and Huang, H., *Experimental study on the effects of hydrogen addition on the emission and heat transfer characteristics of laminar methane diffusion flames with oxygen-enriched air*. International Journal of Hydrogen Energy, 2016. **41**(3): p. 2023-2036, DOI: <https://doi.org/10.1016/j.ijhydene.2015.10.132>.
  - [35]. Hansen, O.R., *Hydrogen infrastructure—Efficient risk assessment and design optimization approach to ensure safe and practical solutions*. Process Safety and Environmental Protection, 2020. **143**: p. 164-176, DOI: <https://doi.org/10.1016/j.psep.2020.06.028>.
  - [36]. Celtek, M.S. and Pinarbaşı, A., *Investigations on performance and emission characteristics of an industrial low swirl burner while burning natural gas, methane, hydrogen-enriched natural gas and hydrogen as fuels*. International journal of hydrogen energy, 2018. **43**(2): p. 1194-1207, DOI: <https://doi.org/10.1016/j.ijhydene.2017.05.107>.
  - [37]. Cho, E.-S. and Chung, S.H., *Improvement of flame stability and NO<sub>x</sub> reduction in hydrogen-added ultra lean premixed combustion*. Journal of mechanical science and technology, 2009. **23**(3): p. 650-658, DOI: <https://doi.org/10.1007/s12206-008-1223-x>.
  - [38]. Rajpara, P., Shah, R., and Banerjee, J., *Effect of hydrogen addition on combustion and emission characteristics of methane fuelled upward swirl can combustor*. International journal of hydrogen energy, 2018. **43**(36): p. 17505-17519, DOI: <https://doi.org/10.1016/j.ijhydene.2018.07.111>.
  - [39]. Guo, H., Smallwood, G.J., Liu, F., Ju, Y., and Gülder, Ö.L., *The effect of hydrogen addition on flammability limit and NO<sub>x</sub> emission in ultra-lean counterflow CH<sub>4</sub>/air premixed flames*. Proceedings of the Combustion Institute, 2005. **30**(1): p. 303-311, DOI: <https://doi.org/10.1016/j.proci.2004.08.177>.
  - [40]. Cano Ardila, F.E., Obando Arbeláez, J.E., and Amell Arrieta, A.A., *Emissions and dynamic stability of the flameless combustion regime using hydrogen blends with natural gas*. International Journal of Hydrogen Energy, 2020. **46**(1), DOI: <https://doi.org/10.1016/j.ijhydene.2020.09.236>.
  - [41]. Kashir, B., Tabejamaat, S., and Jalalati, N., *A numerical study on combustion characteristics of blended methane-hydrogen bluff-body stabilized swirl diffusion flames*. International Journal of Hydrogen Energy, 2015. **40**(18): p. 6243-6258, DOI: <https://doi.org/10.1016/j.ijhydene.2015.03.023>.
  - [42]. Baek, S.W., Ju Kim, J., Kim, H.S., and Kang, S.H., *Effects of Addition of Solid Particles on Thermal Characteristics in Hydrogen-Air Flame*. Combustion science and technology, 2002. **174**(8): p. 99-116, DOI: <https://doi.org/10.1080/00102200290021263>.
  - [43]. Waheed, K., Baek, S.W., Javed, I., and Kristiyanto, Y., *Investigations on Thermal Radiative Characteristics of LPG Combustion: Effect of Alumina Nanoparticles Addition*. Combustion science and technology, 2015. **187**(6): p. 827-842, DOI: <https://doi.org/10.1080/00102202.2014.973952>.
  - [44]. Schumacher, G. and Juniper, L., *Coal utilisation in the cement and concrete industries*, in *The Coal Handbook: Towards Cleaner Production*, D. Osborne, Editor. 2013, Woodhead Publishing. p. 387-426.
  - [45]. Evans, M.J., Proud, D.B., Medwell, P.R., Pitsch, H., and Dally, B.B., *Highly radiating hydrogen flames: Effect of toluene concentration and phase*. Proceedings of the Combustion Institute, 2020. **38**(1), DOI: <https://doi.org/10.1016/j.proci.2020.07.005>.
  - [46]. Dooley, S., Won, S.H., Chaos, M., Heyne, J., Ju, Y., Dryer, F.L., Kumar, K., Sung, C.-J., Wang, H., Oehlschlaeger, M.A., Santoro, R.J., and Litzinger, T.A., *A jet fuel surrogate formulated by real fuel properties*. Combustion and Flame, 2010. **157**(12): p. 2333-2339, DOI: <https://doi.org/10.1016/j.combustflame.2010.07.001>.

- [47]. Pepiot-Desjardins, P., Pitsch, H., Malhotra, R., Kirby, S.R., and Boehman, A.L., *Structural group analysis for soot reduction tendency of oxygenated fuels*. Combustion and Flame, 2008. **154**(1): p. 191-205, DOI: <https://doi.org/10.1016/j.combustflame.2008.03.017>.
- [48]. Katta, V.R., Stouffer, S., and Roquemore, W.M., *Stability of lifted flames in centerbody burner*. Combustion and Flame, 2011. **158**(6): p. 1149-1159, DOI: <https://doi.org/10.1016/j.combustflame.2010.10.022>.
- [49]. Kashif, M., Bonnetty, J., Matynia, A., Da Costa, P., and Legros, G., *Sooting propensities of some gasoline surrogate fuels: Combined effects of fuel blending and air vitiation*. Combustion and Flame, 2015. **162**(5): p. 1840-1847, DOI: <https://doi.org/10.1016/j.combustflame.2014.12.005>.
- [50]. Consalvi, J.-L., Liu, F., Kashif, M., and Legros, G., *Numerical study of soot formation in laminar coflow methane/air diffusion flames doped by n-heptane/toluene and iso-octane/toluene blends*. Combustion and Flame, 2017. **180**: p. 167-174, DOI: <https://doi.org/10.1016/j.combustflame.2017.03.002>.
- [51]. Russo, C., Giarracca, L., Stanzone, F., Apicella, B., Tregrossi, A., and Ciajolo, A., *Sooting structure of a premixed toluene-doped methane flame*. Combustion and Flame, 2018. **190**: p. 252-259, DOI: <https://doi.org/10.1016/j.combustflame.2017.12.004>.
- [52]. Mullinger, P. and Jenkins, B., *Chapter 5 - Flames and Burners for Furnaces*, in *Industrial and Process Furnaces (Second Edition)*, P. Mullinger and B. Jenkins, Editors. 2013, Butterworth-Heinemann: Oxford. p. 139-207.
- [53]. Rowhani, A., Chinnici, A., Evans, M., Medwell, P., Nathan, G., and Dally, B. *Variation of residence time in non-premixed turbulent bluff-body ethylene flames as a function of burner diameter*. in *21st Australasian Fluid Mechanics Conference, Adelaide, Australia, December*. 2018.
- [54]. Masri, A., Kelman, J., and Dally, B. *The instantaneous spatial structure of the recirculation zone in bluff-body stabilized flames*. in *Symposium (International) on Combustion*. 1998. Elsevier, DOI: [https://doi.org/10.1016/S0082-0784\(98\)80503-1](https://doi.org/10.1016/S0082-0784(98)80503-1).
- [55]. Dally, B., Masri, A., Barlow, R., and Fiechtner, G., *Instantaneous and mean compositional structure of bluff-body stabilized nonpremixed flames*. Combustion and Flame, 1998. **114**(1-2): p. 119-148, DOI: [https://doi.org/10.1016/S0010-2180\(97\)00280-0](https://doi.org/10.1016/S0010-2180(97)00280-0).
- [56]. Dally, B.B., Masri, A.R., Barlow, R.S., Fiechtner, G.J., and Fletcher, D.F., *Measurements of  $\text{NO}$  in turbulent non-premixed flames stabilized on a bluff body*. Symposium (International) on Combustion, 1996. **26**(2): p. 2191-2197, DOI: [https://doi.org/10.1016/S0082-0784\(96\)80045-2](https://doi.org/10.1016/S0082-0784(96)80045-2).
- [57]. Dutka, M., Ditaranto, M., and Løvås, T.,  *$\text{NO}_x$  emissions and turbulent flow field in a partially premixed bluff body burner with  $\text{CH}_4$  and  $\text{H}_2$  fuels*. International Journal of Hydrogen Energy, 2016. **41**(28): p. 12397-12410, DOI: <https://doi.org/10.1016/j.ijhydene.2016.05.154>.
- [58]. Mueller, M.E., Chan, Q.N., Qamar, N.H., Dally, B.B., Pitsch, H., Alwahabi, Z.T., and Nathan, G.J., *Experimental and computational study of soot evolution in a turbulent nonpremixed bluff body ethylene flame*. Combustion and Flame, 2013. **160**(7): p. 1298-1309, DOI: <https://doi.org/10.1016/j.combustflame.2013.02.010>.
- [59]. Qamar, N.H., Nathan, G.J., Alwahabi, Z.T., and King, K.D., *The effect of global mixing on soot volume fraction: measurements in simple jet, precessing jet, and bluff body flames*. Proceedings of the Combustion Institute, 2005. **30**(1): p. 1493-1500, DOI: <https://doi.org/10.1016/j.proci.2004.08.102>.
- [60]. AMME. *Bluff-Body Flows and Flames*. 2018; Available from: <https://web.aeromech.usyd.edu.au/thermofluids/bluff.php>.
- [61]. Rowhani, A., Sun, Z., Medwell, P.R., Nathan, G.J., and Dally, B.B., *Soot-flowfield interactions in turbulent non-premixed bluff-body flames of ethylene/nitrogen*. Proceedings of the Combustion Institute, 2021. **38**(1): p. 1125-1132, DOI: <https://doi.org/10.1016/j.proci.2020.06.148>.



- [62]. Masri, A.R., Dibble, R.W., and Barlow, R.S., *Raman-rayleigh measurements in bluff-body stabilised flames of hydrocarbon fuels*. Symposium (International) on Combustion, 1992. **24**(1): p. 317-324, DOI: [https://doi.org/10.1016/S0082-0784\(06\)80042-1](https://doi.org/10.1016/S0082-0784(06)80042-1).
- [63]. Liu, C., Zhang, J., Yang, T., and Ma, Y. *Bluff-Body Flames in Hot and Diluted Environments*. in *ASME Power Conference*. 2018. American Society of Mechanical Engineers, DOI: <https://doi.org/10.1115/POWER2018-7179>.
- [64]. Jarungthammachote, S., *Simplified model for estimations of combustion products, adiabatic flame temperature and properties of burned gas*. Thermal Science and Engineering Progress, 2020. **17**: p. 100393, DOI: <https://doi.org/10.1016/j.tsep.2019.100393>.
- [65]. Robinson, J.W. and Smith, V., *Emission spectra of organic liquids in oxy-hydrogen flames*. Analytica Chimica Acta, 1966. **36**: p. 489-498, DOI: [https://doi.org/10.1016/0003-2670\(66\)80084-3](https://doi.org/10.1016/0003-2670(66)80084-3).
- [66]. Arens, E.E., Youngquist, R.C., and Starr, S.O., *Intensity calibrated hydrogen flame spectrum*. International Journal of Hydrogen Energy, 2014. **39**(17): p. 9545-9551, DOI: <https://doi.org/10.1016/j.ijhydene.2014.04.043>.
- [67]. Lieuwen, T., Shanbhogue, S., Khosla, S., and Smith, C., *Dynamics of Bluff Body Flames Near Blowoff*. Collection of Technical Papers - 45th AIAA Aerospace Sciences Meeting, 2007. **3**, DOI: 10.2514/6.2007-169.
- [68]. Morales, A.J., Lasky, I.M., Geikie, M.K., Engelmann, C.A., and Ahmed, K.A., *Mechanisms of flame extinction and lean blowout of bluff body stabilized flames*. Combustion and Flame, 2019. **203**: p. 31-45, DOI: <https://doi.org/10.1016/j.combustflame.2019.02.002>.
- [69]. Kim, S.-H., Kim, M., Yoon, Y., and Jeung, I.-S., *The effect of flame radiation on the scaling of nitrogen oxide emissions in turbulent hydrogen non-premixed flames*. Proceedings of the Combustion Institute, 2002. **29**(2): p. 1951-1956, DOI: [https://doi.org/10.1016/S1540-7489\(02\)80237-1](https://doi.org/10.1016/S1540-7489(02)80237-1).
- [70]. Kim, S.-H., Yoon, Y., and Jeung, I.-S., *Nitrogen oxides emissions in turbulent hydrogen jet non-premixed flames: Effects of coaxial air and flame radiation*. Proceedings of the Combustion Institute, 2000. **28**(1): p. 463-471, DOI: [https://doi.org/10.1016/S0082-0784\(00\)80244-1](https://doi.org/10.1016/S0082-0784(00)80244-1).
- [71]. Cai, L. and Pitsch, H., *Optimized chemical mechanism for combustion of gasoline surrogate fuels*. Combustion and Flame, 2015. **162**(5): p. 1623-1637, DOI: <https://doi.org/10.1016/j.combustflame.2014.11.018>.
- [72]. Violi, A., D'Anna, A., and D'Alessio, A., *Modeling of particulate formation in combustion and pyrolysis*. Chemical Engineering Science, 1999. **54**(15-16): p. 3433-3442.
- [73]. Dally, B., Fletcher, D., and Masri, A., *Flow and mixing fields of turbulent bluff-body jets and flames*. Combustion Theory and Modelling, 1998. **2**(2): p. 193.
- [74]. Deng, S., Mueller, M.E., Chan, Q.N., Qamar, N.H., Dally, B.B., Alwahabi, Z.T., and Nathan, G.J., *Hydrodynamic and chemical effects of hydrogen addition on soot evolution in turbulent nonpremixed bluff body ethylene flames*. Proceedings of the Combustion Institute, 2017. **36**(1): p. 807-814, DOI: <https://doi.org/10.1016/j.proci.2016.09.004>.
- [75]. Kang, Y.-H., Wang, Q.-H., Lu, X.-F., Ji, X.-Y., Miao, S.-S., Wang, H., Guo, Q., He, H.-H., and Xu, J., *Experimental and theoretical study on the flow, mixing, and combustion characteristics of dimethyl ether, methane, and LPG jet diffusion flames*. Fuel Processing Technology, 2015. **129**: p. 98-112, DOI: <https://doi.org/10.1016/j.fuproc.2014.09.004>.
- [76]. Gülder, Ö.L., Snelling, D.R., and Sawchuk, R.A., *Influence of hydrogen addition to fuel on temperature field and soot formation in diffusion flames*. Symposium (International) on Combustion, 1996. **26**(2): p. 2351-2358, DOI: [https://doi.org/10.1016/S0082-0784\(96\)80064-6](https://doi.org/10.1016/S0082-0784(96)80064-6).
- [77]. Mueller, M.E. and Pitsch, H., *Large eddy simulation of soot evolution in an aircraft combustor*. Physics of Fluids, 2013. **25**(11): p. 110812, DOI: <https://doi.org/10.1063/1.4819347>.

- [78]. Evans, M.J., Medwell, P.R., Sun, Z., Chinnici, A., Ye, J., Chan, Q.N., and Dally, B.B., *Downstream evolution of n-heptane/toluene flames in hot and vitiated coflows*. Combustion and Flame, 2019. **202**: p. 78-89, DOI: <https://doi.org/10.1016/j.combustflame.2019.01.008>.
- [79]. Liu, F., Guo, H., Smallwood, G.J., and Gülder, Ö.L., *Effects of gas and soot radiation on soot formation in a coflow laminar ethylene diffusion flame*. Journal of Quantitative Spectroscopy and Radiative Transfer, 2002. **73**(2): p. 409-421, DOI: [https://doi.org/10.1016/S0022-4073\(01\)00205-9](https://doi.org/10.1016/S0022-4073(01)00205-9).
- [80]. Wang, X., Jin, Q., Zhang, J., Li, Y., Li, S., Mikulčić, H., Vujanović, M., Tan, H., and Duić, N., *Soot formation during polyurethane (PU) plastic pyrolysis: The effects of temperature and volatile residence time*. Energy Conversion and Management, 2018. **164**: p. 353-362, DOI: <https://doi.org/10.1016/j.enconman.2018.02.082>.
- [81]. Smooke, M.D., Long, M.B., Connelly, B.C., Colket, M.B., and Hall, R.J., *Soot formation in laminar diffusion flames*. Combustion and Flame, 2005. **143**(4): p. 613-628, DOI: <https://doi.org/10.1016/j.combustflame.2005.08.028>.
- [82]. Kronenburg, A., Bilger, R.W., and Kent, J.H., *Modeling soot formation in turbulent methane-air jet diffusion flames*. Combustion and Flame, 2000. **121**(1): p. 24-40, DOI: [https://doi.org/10.1016/S0010-2180\(99\)00146-7](https://doi.org/10.1016/S0010-2180(99)00146-7).
- [83]. Sutherland, J.C., Smith, P.J., and Chen, J.H., *Quantification of differential diffusion in nonpremixed systems*. Combustion Theory and Modelling, 2005. **9**(2): p. 365-383, DOI: <https://doi.org/10.1080/17455030500150009>.
- [84]. Yen, M., Magi, V., and Abraham, J., *Modeling the effects of hydrogen and nitrogen addition on soot formation in laminar ethylene jet diffusion flames*. Chemical Engineering Science, 2019. **196**: p. 116-129, DOI: <https://doi.org/10.1016/j.ces.2018.07.061>.
- [85]. Migliorini, F., *Study of combustion process of hydrogen-hydrocarbon mixtures*. 2008, Politecnico di Milano.
- [86]. Ji, W., Yang, T., Ren, Z., and Deng, S., *Dependence of kinetic sensitivity direction in premixed flames*. Combustion and Flame, 2020. **220**: p. 16-22, DOI: <https://doi.org/10.1016/j.combustflame.2020.06.027>.
- [87]. Xie, S., Lu, Z., and Chen, Z., *Effects of strain rate and Lewis number on forced ignition of laminar counterflow diffusion flames*. Combustion and Flame, 2021. **226**: p. 302-314, DOI: <https://doi.org/10.1016/j.combustflame.2020.12.027>.
- [88]. Vagelopoulos, C. and Egolfopoulos, F., *Laminar flame speeds and extinction strain rates of mixtures of carbon monoxide with hydrogen, methane, and air*. Symposium (international) on Combustion, 1994. **25**(1): p. 1317-1323, DOI: [https://doi.org/10.1016/S0082-0784\(06\)80773-3](https://doi.org/10.1016/S0082-0784(06)80773-3).
- [89]. Kent, J.H. and Bastin, S.J., *Parametric effects on sooting in turbulent acetylene diffusion flames*. Combustion and Flame, 1984. **56**(1): p. 29-42, DOI: [https://doi.org/10.1016/0010-2180\(84\)90003-8](https://doi.org/10.1016/0010-2180(84)90003-8).
- [90]. Coriton, B., Smooke, M.D., and Gomez, A., *Effect of the composition of the hot product stream in the quasi-steady extinction of strained premixed flames*. Combustion and Flame, 2010. **157**(11): p. 2155-2164, DOI: <https://doi.org/10.1016/j.combustflame.2010.05.002>.